2024 International Conference on Quantum Communications, Networking, and Computing (QCNC) | 979-8-3503-6677-8/24/$31.00 ©2024 IEEE | DOI: 10.1109/QCNC62729.2024.00029

Quantum LAN: On-Demand Network Topology via Two-colorable Graph States

Francesco Mazza, Marcello Caleffi, *Senior Member, IEEE*, Angela Sara Cacciapuoti, *Senior Member, IEEE*

***Abstract*—In Quantum Local Area Networks (QLANs) – the near-term building block of the Quantum Internet – the choice of the physical network topology is not so restrictive and binding as in classical LAN in terms of communication capabilities among the network nodes. And the rationale for this is the entanglement-enabled connectivity induced by multipartite entangled states. Indeed, it is possible to create on-demand links between the QLAN nodes by properly manipulating the shared multipartite entangled states. Thus, it is possible to build an overlay entangled network upon the physical one, characterized by a topology different from the physical one and referred to as *artificial topology*. In this paper we address the fundamental issue of engineering the artificial topology to bypass the limitations induced by the physical network topology. This possibility to overcome the constraints in the network design induced by the physical topology has no counterpart in classical networks. To this aim, we exploit the properties of a class of multipartite entangled states, referred to as graph states, which exhibit unique properties, making them very interesting and promising for engineering artificial topologies in QLANs.**

***Index Terms*—Local Area Network(LAN), Quantum LAN, Multipartite Entanglement, Graph states, Network Topology.**

I. Introduction

In its final stage, the Quantum Internet is envisioned as a global interconnection of heterogeneous quantum networks, able to transmit quantum bits (qubits) and to distribute entangled quantum states with no classical equivalent [1]–[5].

In a shorter-term time-horizon, given the current technology-readiness level, interconnecting different quantum processors with a Quantum Local Area Network (QLAN) – namely, with a quantum network able to cover a limited geographic area – represents one of the very first steps for unlocking the vision of the Quantum Internet. And, indeed, first deployments of quantum server farms are already in place [6], [7].

For an effective QLAN design, it is crucial to account for the new and richer form of connectivity enabled by entanglement [3], [8], which has no-counterpart in classical networks. Specifically, once an entangled state - say an EPR pair for the sake of exemplification – has been shared between two nodes, a qubit can be "transmitted" via quantum teleportation [9], [10], regardless of the instantaneous conditions of the physical quantum link connecting the two nodes. Remarkably, qubit transmission is still possible even when there is no longer a quantum link connecting the nodes together. In this sense, entanglement enables a new form of connectivity, referred to as *entanglement-enabled connectivity*. Furthermore, entanglement can be swapped and, hence, it is possible to change the identities of the entangled nodes at run-time, by redefining the very same concept of topological neighborhood with no counterpart in the classical world. Accordingly, entanglement enables half-duplex unicast links between any pairs of nodes, regardless of their relative positions within the **underlying physical network topology**. Hence, any pair of nodes can be neighbor as long as they share entanglement.

Additionally, entanglement is not limited to EPR pairs. With multipartite entanglement [11], [12], the dynamic nature of the entanglement-based connectivity becomes even more evident and richer. For instance, by distributing an n-qubit GHZ state [11] among n network nodes, an EPR pair can be distributively extracted by any pair of nodes, with the identities of the entangled nodes chosen at run-time.

From the above, it is evident that the choice of the physical topology of a QLAN is not so restrictive as in classical LANs in terms of communication capabilities among the network nodes. Indeed, as exemplified in the above examples, the node communication capabilities go beyond the physical topology due to the marvels of the entanglement-based connectivity.

Consequently, it is possible to create *artificial links*[1] between the QLAN nodes on-demand, by properly manipulating the shared multipartite entangled states. These artificial links constitute a sort of "overlay entangled network" built upon the physical one, and characterized by a topology – referred to as *artificial topology* – that can differs significantly from the physical one.

In this paper, we shed light on the possibility of engineering the artificial QLAN topology to overcome the limitations and the communication constraints induced by the physical QLAN topology. This possibility has no counterpart in classical networks.

The authors are with the www.QuantumInternet.it research group, *FLY: Future Communications Laboratory*, University of Naples Federico II, Naples, 80125 Italy. A.S. Cacciapuoti and M. Caleffi are also with the Laboratorio Nazionale di Comunicazioni Multimediali, National Inter-University Consortium for Telecommunications (CNIT), Naples, 80126, Italy.

Angela Sara Cacciapuoti and Francesco Mazza acknowledge PNRR MUR NQSTI-PE00000023, Marcello Caleffi acknowledges PNRR MUR project RESTART-PE00000001.

[1]It may be useful to clarify that an artificial link between two network nodes denotes the "possibility" of extracting a shared EPR between the two nodes, starting from a multipartite entangled state shared among a larger set of nodes. However, the number of EPR pairs that can be simultaneously extracted from a single multipartite entangled state heavily depends on the type and structure of the considered state [13], and some of the artificial links are depleted during the extraction process.

979-8-3503-6677-8/24/$31.00 ©2024 IEEE
DOI 10.1109/QCNC62729.2024.00029

To this aim, we exploit the properties of a class of multipartite entangled states, referred to as *graph states* [14], that recently gained significant attention from the community [15]–[19] due to their unique entanglement properties [13], [14]. Indeed such properties make graph states ideal resources for various applications in quantum computing and quantum communications.

We focus on a specific[2] class of graph states, namely, *two-colorable* graph states, since they exhibit regular structures and we engineer this regularity by exploiting different degrees of freedom, including the number of communication qubits [20] available in the QLAN. Our findings show that – by exploiting local operations only at the central node of a *star* physical topology – it is possible to engineer the artificial topology among the QLAN nodes for overcoming the physical topological constraints.

The remaining part of the manuscript is organized as follows. In Sec. II, we introduce some preliminaries related to classical LAN and graph states. In Sec. III, we first describe the system model, and then we develop the theoretical analysis by providing the tools for engineering the artificial topology beyond the limitations induced by the physical one. Finally, in Sec. IV, we conclude the paper.

II. Preliminaries

In this section, we first introduce in Sec. II-A basic concepts related to classical LANs and their topologies, providing so essential concepts and vocabulary used in the following. Then, in Sec. II-B, we briefly overview some notions related to graph theory, which will be used in Sec. II-C to present and describe a key class of multipartite entangled states – namely, the *graph states* – and the main tools for their manipulation. Specifically, we describe how the edges of the graph associated to a *graph state* can be modified by exploiting local operations only.

A. Local Area Networks

Classical Local Area Networks (LANs) are communication networks designed to cover limited geographic areas. Historically, they served as a mean to share resources, such as files, printers and lately internet connections, among networked nodes.

Traditionally, the choice of the physical LAN topology interconnecting the nodes has been crucial, since the (subsequent) design of the LAN communication protocols – and, hence, the overall LAN performances – strictly depends on such a choice[3]. As a matter of fact, the choice of the physical topology anticipates the actual LAN deployment, and it remains fixed regardless of any changes or evolution of the LAN communication needs. Hence, the structure and functionality of LANs have undergone several evolutions over the years, seeking to improve the adaptability and scalability of the network. Among the reference LAN topologies, we can mention three archetypes: *bus*, *ring*, and *star*, briefly overviewed in the following.

1) **Bus topology**. In a bus topology, a single medium (e.g., a coaxial cable) is shared among all the LAN nodes. Although cost-effective and easy to install, the bus topology introduces a point-of-failure vulnerability: whenever the bus fails, the entire LAN experiences service disruption. The bus topology was adopted within the original IEEE 802.3 standards, defining the *physical* and *data-link* layers for wired Ethernet [21].
2) **Ring topology**. Another noteworthy LAN physical topology is the ring topology, where each node communicates with exactly two neighboring nodes. Data travels along the ring, passing from one device to the next one until reaching its destination [22], [23]. Despite offering significant advantages over bus (such as simple routing algorithms), a ring topology cannot tolerate the failure of neither the bus nor any single node, and it pose significant deployment challenges when it comes to network expansion.
3) **Star topology**. Widely adopted in late-Ethernet and WiFi networks [24], it enforces each LAN node to be connected to a central hub (aka as *hub*/*switch* in Ethernet and *access point* in WiFi terminologies). All data traffic is directed through the hub, which can serve as a central control point for the entire LAN. While introducing the possibility of centralized management and scalability – simplifying so network administration and troubleshooting as well as network expansion – star topologies also suffer from the problem of a single point of failure, yet limited to the hub.

It is clear from the above that not only the LAN deployment, but also the design of any LAN protocol must take into account – since the very initial stages – the pros and cons offered by the actual choice of the underlying physical topology.

Conversely, as we will show in Sec. III, the choice of the physical topology of a QLAN is not so restrictive as in classical LAN in terms of communication capabilities among the network nodes, since it is possible to create artificial on-demand links between the QLAN nodes.

B. Graph theory fundamentals

Before introducing *graph states* and their properties in Sec. II-C, it is convenient to overview some basic definitions and notations from classical graph theory. Formally, a graph[4] G is defined as:

$$G \triangleq (V, E), \tag{1}$$

[2]It is worthwhile to note that our assumption of relying on two-colorable states is not restrictive, since any graph state can be converted in a two-colorable one under very relaxed conditions as discussed in Sec III.

[3]With a representative example given by the radical differences in the Medium Access Control (MAC) protocol design when it comes to *bus* vs *ring* topologies.

[4]In the following, we will restrict our attention on finite graphs, i.e., graphs with finite set of vertices and edges. Furthermore, we will consider *undirected*, *simple* graphs only, since these two properties are required for the mapping between graphs and graph states [13], [14].

with V denoting the set of vertices – also called *nodes* – with cardinality $|V| = n$, and E denoting the set of edges that describes the connections between the vertices:

$$E \subset V \times V \triangleq [V]^2 \triangleq \{\{a,b\} : a,b \in V \wedge a \neq b\}. \quad (2)$$

A graph can be pictorially represented by a diagram in a plane, where each vertex is denoted by a point and each edge is denoted by an arch between two nodes.

Given two vertices $a, b \in V$, if a and b are connected through an edge $\{a,b\} \in E$, then they are defined as *adjacent* vertices. The set of vertices adjacent to a given vertex a is called *neighborhood* of a, and it is defined as:

$$N_a = \{b \in V | \{a,b\} \in E\}. \quad (3)$$

In particular, a vertex a such that $|N_a| = 0$ is called *isolated vertex*. Stemming from the concept of *neighborhood*, it is possible to introduce the notion of *subgraph induced by a neighborhood*. Specifically, the subgraph of G induced by N_a is the graph having: i) as vertices, the ones in N_a, and ii) as edges, the edges in E whose endpoints are both in N_a. Formally:

$$G[N_a] = (N_a, E_{N_a}), \quad (4)$$

with $E_{N_a} \triangleq \{\{b,c\} \in E : b \in N_a \wedge c \in N_a\} = E \cap [N_a]^2$.

An important operation on graphs for the purpose of this paper is *graph complementation*, which is defined as follows. The complement (or inverse) of a graph G is the graph $\tau(G)$, obtained by considering the same set of vertices V but with the edge set built such that two distinct vertices of $\tau(G)$ are adjacent if and only if they are not adjacent in G. Formally:

$$\tau(G) = (V, E^C) \quad (5)$$

with $E^C \triangleq [V]^2 \setminus E = \{\{a,b\} \in [V]^2 : \{a,b\} \notin E\}$. The complementation can be done also with respect to the subgraph $G[N_a]$ of G induced by N_a. In this case, it is usually referred as *local complementation* of G at vertex a, and it is denoted as $\tau_a(G)$. More into details, $\tau_a(G)$ is obtained by complementing the subgraph of G induced by the neighborhood N_a while leaving the rest of the graph unchanged:

$$\tau_a(G) = (V, E \cup [N_a]^2 \setminus E_{N_a}) \quad (6)$$

Vertex deletion is another graph operation used in the following. Specifically, deleting vertex a in graph G generates a new graph $G - a$ where both vertex a and all the edges connecting a with its adjacent vertexes are removed. Formally:

$$G - a = \big(V \setminus \{a\}, E \setminus E_a\big) \quad (7)$$

with $E_a \triangleq \big\{\{a,b\} \in E : b \in N_a\big\}$, denoting the set of edges between a and its adjacent vertexes.

C. Graph states

A notable (from a communication perspective) class of multipartite entangled states is represented by the so-called *graph states* [13], [14], which – as suggested by the name – can be effectively described with the graph theory tools introduced in Sec.II-B.

Specifically, stemming from an arbitrary graph G defined in (1), the corresponding *graph state* $|G\rangle$ is obtained by mapping each vertex of the graph G with a qubit in the state $|+\rangle$, and then performing a controlled-Z ($\mathtt{CZ}$) gate between each pair of qubits corresponding to adjacent vertices in G.

Remark. *The rationale underlying such a mapping lies in the correspondence between graph edges and interaction patterns among the qubits belonging to the composite – entangled – system. In the mapping, vertices play the role of physical systems and edges represent their interactions.*

Formally, the *graph state* $|G\rangle$ associated to $G \triangleq (V, E)$ can be expressed[5] as [13]:

$$|G\rangle = \prod_{\{a,b\} \in E} \mathtt{CZ}_{ab} \, |+\rangle^{\otimes n} \quad (8)$$

with $|+\rangle = \frac{1}{\sqrt{2}}(|0\rangle + |1\rangle)$, $n = |V|$ and $\mathtt{CZ}_{ab}$ denoting the Controlled-Z ($\mathtt{CZ}$) gate applied to the qubits associated to the vertices a and b.

The above mapping between graph states and graphs is crucial beyond a merely pictorial purpose. Specifically, the action of key operations on a graph state $|G\rangle$ can be described via simple transformations on the associated graph G. Among these transformations, single-qubit Pauli measurements play a crucial role for the objectives of this paper.

More into details, a projective measurement through a Pauli operator σ_x, σ_y, or σ_z on a qubit of the graph state $|G\rangle$ yields, up to local unitaries $U_{i,\pm}$, a new graph state $|\tilde{G}\rangle$ on the unmeasured qubits. Interestingly, as proved in [13], [14], this new graph state $|\tilde{G}\rangle$ can be obtained by means of simple transformations on the graph G associated to the original graph state $|G\rangle$, such as vertex deletion and the local complementation introduced in (6) and (7), respectively.

Since these projective measurements will be exploited in Sec. III for engineering the artificial topology enabled by entanglement, it is convenient to summarize in the following their effects on an arbitrary graph state $|G\rangle$.

i) **Projective measurement via Pauli operator σ_z:** The measurement of a qubit – associated to vertex a in graph G – of the initial graph state $|G\rangle$ yields, up to local unitaries, to a new graph state $|\tilde{G}_z\rangle$[6] among the remaining

[5] With a (widely adopted) notation abuse, since the application of the $\mathtt{CZ}_{ab}$ gate on the state $|+\rangle^{\otimes n}$ requires a reference to $n-2$ identity operations I acting on all the qubits different from a or b.

[6] With a mild notation abuse, the dependence on a is neglected for the sake of notation simplicity. Similar notation abuses will be adopted also for the following projective measurements.

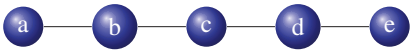

(a) Representation of the graph G associated to a 5-qubits *linear* graph state $|G\rangle$.

(b) Representation of the graph $\tilde{G}_z = G - c$ obtained by performing a σ_z-measurement on the qubit associated to vertex c.

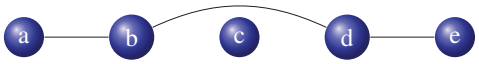

(c) Representation of the graph $\tilde{G}_y = \tau_c(G) - c$ obtained by performing a σ_y-measurement on the qubit associated to vertex c.

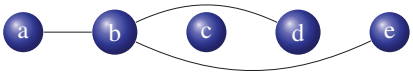

(d) Representation of the graph $\tilde{G}_x = \tau_d(\tau_c(\tau_d(G) - c))$ obtained by performing a σ_x-measurement on the qubit associated to vertex c.

Fig. 1: Pictorial representation of the effects of different single-qubit Pauli-measurements on a graph state. The effects are shown by representing the graph associated with the graph state obtained after the measurements (up to local unitaries).

qubits, whose associate graph $\tilde{G}_z$ is obtained by deleting the vertex a from graph G. Formally:

$$\tilde{G}_z \triangleq G - a, \tag{9}$$

$$P^{(a)}_{z,\pm} |G\rangle = |z,\pm\rangle^{(a)} \otimes \underbrace{U^{(a)}_{z,\pm} |G-a\rangle}_{\triangleq |\tilde{G}_z\rangle}, \tag{10}$$

with $P^{(a)}_{z,\pm}$ denoting the projector of qubit a onto the eigenvector $|z,\pm\rangle^{(a)}$ of $\sigma_z^{(a)}$ with eigenvalues ± 1, and $U^{(a)}_{z,\pm}$ denoting the correcting unitary, whose expression depends on the measurement outcome[7]:

$$U^{(a)}_{z,+} = \mathbb{I}, \qquad U^{(a)}_{z,-} = \bigotimes_{b \in N_a} \sigma_z^{(b)}. \tag{11}$$

ii) **Projective measurement via Pauli operator σ_y:** The measurement of a qubit – associated to vertex a in graph G – of the initial graph state $|G\rangle$ yields, up to local unitaries, to a new graph state $|\tilde{G}_y\rangle$ among the remaining qubits, whose associate graph $\tilde{G}_y$ is obtained: i) first, by local complementation of the graph G at vertex a, and ii) then, by deleting a from graph G. Formally:

$$\tilde{G}_y \triangleq \tau_a(G) - a, \tag{12}$$

$$P^{(a)}_{y,\pm} |G\rangle = |y,\pm\rangle^{(a)} \otimes \underbrace{U^{(a)}_{y,\pm} |\tau_a(G) - a\rangle}_{\triangleq |\tilde{G}_y\rangle}, \tag{13}$$

with $P^{(a)}_{y,\pm}$ denoting the projector of qubit a onto the eigenvector $|y,\pm\rangle^{(a)}$ of $\sigma_y^{(a)}$ with eigenvalues ± 1, and $U^{(a)}_{y,\pm}$ denoting the correcting unitary, whose expression depends on the measurement outcome:

$$U_{y,+} = \bigotimes_{b \in N_a} \sqrt{-i\sigma_z^{(b)}}, \qquad U_{y,-} = \bigotimes_{b \in N_a} \sqrt{i\sigma_z^{(b)}}. \tag{14}$$

iii) **Projective measurement via Pauli operator σ_x:** The measurement of the arbitrary qubit – associated to vertex a in graph G – of the initial graph state $|G\rangle$ yields, up to local unitaries, to a new graph state $|\tilde{G}_x\rangle$ among the remaining qubits, whose associate graph $\tilde{G}_x$ is obtained by concatenating the following three graph operations: i) local complementation of the graph G at an arbitrary neighbor vertex $b_0 \in N_a$, ii) then, local complementation of the graph G at vertex a, followed by the deletion of a from graph G, and iii) finally, a local complementation at b_0 of the graph obtained at the previous step. Formally:

$$\tilde{G}_x = \tau_{b_0}\big(\tau_a(\tau_{b_0}(G)) - a\big), \tag{15}$$

$$P^{(a)}_{x,\pm} |G\rangle = |x,\pm\rangle^{(a)} \otimes \underbrace{U^{(a)}_{x,\pm} |\tau_{b_0}\left(\tau_a\left(\tau_{b_0}(G)\right) - a\right)\rangle}_{\triangleq |\tilde{G}_x\rangle}, \tag{16}$$

with $P^{(a)}_{x,\pm}$ denoting the projector of qubit a onto the eigenvector $|x,\pm\rangle^{(a)}$ of $\sigma_x^{(a)}$ with eigenvalues ± 1, and $U^{(a)}_{x,\pm}$ denoting the correcting unitary, whose expression depends on the measurement outcome:

$$U_{x,+} = \sqrt{i\sigma_y^{(b_0)}} \bigotimes_{b \in N_{b_0} \setminus \{N_a \cup \{a\}\}} \sigma_z^{(b)}, \tag{17}$$

$$U_{x,-} = \sqrt{-i\sigma_y^{(b_0)}} \bigotimes_{b \in N_{b_0} \setminus \{N_a \cup \{a\}\}} \sigma_z^{(b)}.$$

It is worthwhile to note that, although the choice of the vertex b_0 in the neighbourhood of a at step i) is not unique, the post-measurement graph states are LU equivalent for any choice of b_0 [13].

In Fig. 1 we represent the effects of the three different Pauli measurements on a graph state through the changes in the corresponding associated graph.

III. From Physical to Artificial Topology

In this section, we exploit the tools introduced in Sec. II to show how the artificial QLAN topology can be engineered from a communication perspective to overcome the limitations of the physical QLAN topology.

[7]With a (widely adopted in literature) notation abuse, since the expression of $U^{(a)}_{z,-}$ would require a reference to $n - |N_a| - 1$ identity operations $\mathtt{I}$ acting on all the qubits not belonging to the neighbourhood of a. Similar notation abuses will be adopted also later in the paper.

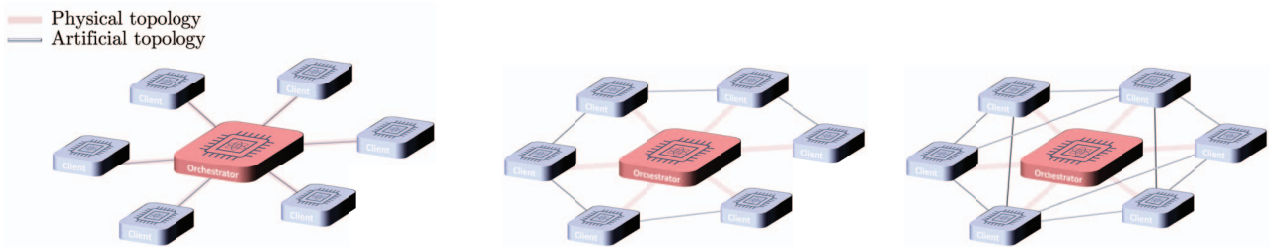

(a) (b) (c)

Fig. 2: Pictorial representation of a QLAN. The orchestrator node (shown in red) is connected to the client nodes via a physical topology. After operations performed locally at the orchestrator, artificial topologies are built upon the physical one: artificial bus topology, in the sub-figure (b) or artificial (enhanced) ring topology, in the sub-figure (c).

A. System Model

In many practical scenarios, the generation of multipartite entanglement requires sophisticated and resource-intensive setups, often involving complex experimental apparatuses and precise control mechanisms.

This makes pragmatic to assume a specialized super-node, referred to as *orchestrator* in the following, responsible for locally generating and then distributing a multipartite entangled state – and, specifically, a graph state in our case – among the network nodes [25]–[27]. To this aim, the orchestrator is directly connected through physical quantum channels to each of the network nodes, referred to as *clients* in the following and whose number is assumed equal to k.

Remark. *The assumption of a hierarchy among the nodes, with the orchestrator responsible for distributing the multipartite entanglement state to the client, is clearly realistic, given the current maturity of the quantum technologies and given the unavoidable requirement of some sort of local interaction among the qubits to be entangled. Yet, it imposes a hard constraint on the admissible physical QLAN topology, which is compelled to be a star topology, as illustrated in Fig. 2.*

Luckily – and differently from classical LANs – the physical QLAN topology does not strictly and uniquely determines the communication capabilities of the client nodes. And the reason is that arbitrary on-demand artificial topologies can be built upon the physical one, as shown in the next subsections by exploiting peculiar properties of the graph states.

In this context, we can exploit different degrees of freedom to engineer the artificial topology.

First, it must be acknowledged that a key role is played by i) the number n_o of qubits of the n-qubit graph state retained by the orchestrator, and ii) the number of qubits of the graph state distributed at each client node. In the following, we consider the worst-case scenario from a communication perspective: a single entangled qubit distributed at each client. Accordingly, $n = n_o + k$ and the set of vertices of the graph G associated to the graph state $|G\rangle$ can be denoted as

$$V = \{o_1, \dots o_{n_o}, c_1, \dots c_k\} \tag{18}$$

with o_i and c_j denoting the vertices associated with the i-th qubit at the orchestrator and the qubit at the j-th client, respectively.

Remark. *As an example of the key role played by these qubit numbers, let us consider a n-qubit graph state with $n = 1+k$. Under this assumption, we have that the number of qubits at the orchestrator is forced to be $n_o = 1$, as depicted in Fig. 2-(a). Hence, if we want to distribute a graph state whose graph is reminiscent of the underlying physical topology – namely, a star topology – we must have $E = \left\{\{o_1, c_i\}_{i=1}^{k}\right\}$. Being the considered graph state LU-equivalent to a GHZ state [13], it allows only the (deterministic) extraction of a single EPR pair between a pair of nodes (i.e., between a couple of clients or between a client and the orchestrator). From this simple example, it appears clear that different choices about n_o imply different features of the resulting graph state and hence of the associated graph, which in turn determine the clients communication capabilities beyond the physical topology constraint. This will be engineered in the next section.*

Another key degree of freedom in the network design is represented by the specific structure of the graph associated to the corresponding graph state[8]. We restrict our attention on two different designed structures of graph states, named in the following as *chain* and *diamond* states, respectively. The choice is not arbitrary, as detailed below.

Indeed, both the two considered structures can be obtained starting from one of the simplest form of graph states – namely, *linear cluster states* – that have been successfully generated in controlled environments [19], [28]. Formally, a linear cluster state is a particular type of graph state, which can be expressed through a simplified expression of (8) as:

$$|C\rangle = \prod_{i=1}^{n-1} \mathrm{CZ}_{(i,i+1)} \, |+\rangle^{\otimes n} \tag{19}$$

Furthermore, both the two graph states can be generated by wisely (as detailed in the next subsections) distributing

[8]Each graph state $|G\rangle$ corresponds uniquely to a graph G. However, graph states associated to different graphs might be equal up to some local unitary (LU) operation [13], [14].

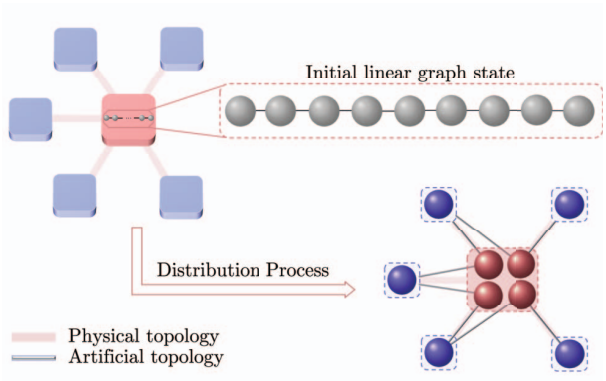

Fig. 3: Pictorial representation of a *chain graph state*, obtained by first generating at the orchestrator a linear cluster state, and then by distributing the entangled qubits to the client so that any qubit retained at the orchestrator is adjacent to two qubits distributed at two different clients.

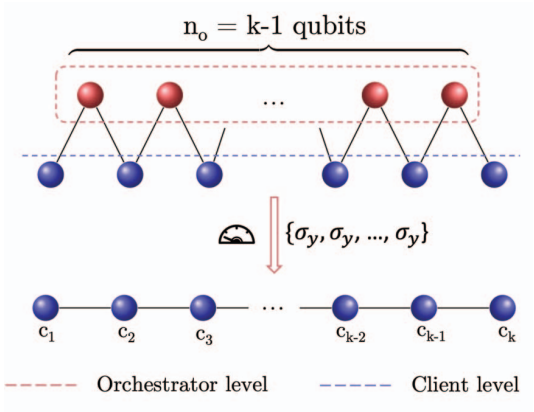

Fig. 4: Generation of an artificial bus topology among the k clients starting from a $(2k-1)$-qubit chain state. In particular, the artificial topology is obtained by (wisely) measuring each qubit retained at the orchestrator.

some qubits of a linear state to the clients, while retained the remaining ones at the orchestrator. Finally, both the two structures belong to the broader and widely investigated family of *two-colorable* graph states. Graph states belong to this family when the associated graph $G = (V, E)$ is bipartite, i.e., vertices can be partitioned into two disjoint subsets so that no pair of vertices within any of the two sets are connected by an edge. Formally:

$$\begin{aligned} &\exists\, V_A, V_B \subseteq V : \\ &\quad V_A \cup V_B = V \ \wedge\ V_A \cap V_B = \emptyset \\ &\quad \wedge\, \forall \{a,b\} \in E : a \in V_A \Longrightarrow b \in V_B \end{aligned} \tag{20}$$

Two-colorable graph states have been widely investigated and they exhibit useful properties [29]. Notable multipartite entangled states – including Greenberger-Horne- Zeilinger (GHZ) states, cluster states and Calderbank-Shor-Steane (CSS) states are two-colorable graph states [14], [30]. It is worthwhile to note that the assumption of having a two-colorable graph state is not restrictive, since a graph is two-colorable if and only if it does not contain any cycle of odd length [13].

B. From Physical Star Topology to Artificial Bus Topology

Definition 1 (Chain graph state)**.** *We define as "chain graph state" a two-colorable graph state with $n = 2k-1$ qubits, whose associated graph $G = (V, E)$ is so that:*

$$\begin{aligned} &V = V_A \cup V_B \,\text{with}\, V_A = \{o_i\}_{i=1}^{k-1} \ \wedge\ V_B = \{c_i\}_{i=1}^{k} \\ &E \subset [V]^2 \text{with}\, E = \bigcup_{i=1}^{k-1} \big\{\{o_i, c_i\}, \{o_i, c_{i+1}\}\big\}. \end{aligned} \tag{21}$$

We note that a chain graph can be easily obtained by generating at the orchestrator a $(2k-1)$-qubits linear cluster state and by wisely distributing some qubits to the clients. Specifically, the qubits to be retained and those to be distributed are interleaved within the linear cluster state, so that any qubit retained at the orchestrator is adjacent (within the original linear topology) to two qubits distributed at two different clients, as illustrated in Fig. 3.

Stemming from this entangled resource is possible to built upon the physical topology an artificial bus topology among the client nodes, by performing a number of Pauli σ_y measurements equal to the number $n_o = k-1$ of orchestration vertices, as established by Lemma 1 and shown in Fig. 4.

Lemma 1. *Given a chain graph state with a number of qubits equal to $n = 2k-1$, with k denoting the number of clients, an artificial bus topology among the k clients can be obtained by performing $k-1$ local σ_y-Pauli measurements on the qubits retained at the orchestrator.*

Proof: The proof follows straightforwardly by first applying local complementation of the graph G – associated to the chain graph state – at vertices $\{o_i\}_{i=1}^{n_o}$ and then by deleting these vertices from the resulting graph, as indicated in (12) *and* (13)*. Thus, the artificial topology obtained from the n-qubit graph state is expressed via the resulting graph $\tilde{G}_y^{(n_o)} = (V_y, E_y)$ with:*

$$V_y = V \setminus V_A = V \setminus \bigcup_{i=1}^{k-1} \{o_i\} \tag{22}$$

$$E_y = \big\{\{c_i, c_{i+1}\} : i = 1, \ldots k-1\big\} \tag{23}$$

■

Remark. *It is worthwhile to note that the artificial bus topology enables*[9] *the simultaneous extraction of a number of EPRs greater than 1, as established in [13]. Thus, this artificial topology enables the possibility to fulfill up to $\lfloor \frac{k}{2} \rfloor$ different client communication needs in parallel (depending on the identities of the clients aiming at communicate each other), through for example the teleporting protocol.*

[9]Clearly, whenever the number of clients is $k > 2$.

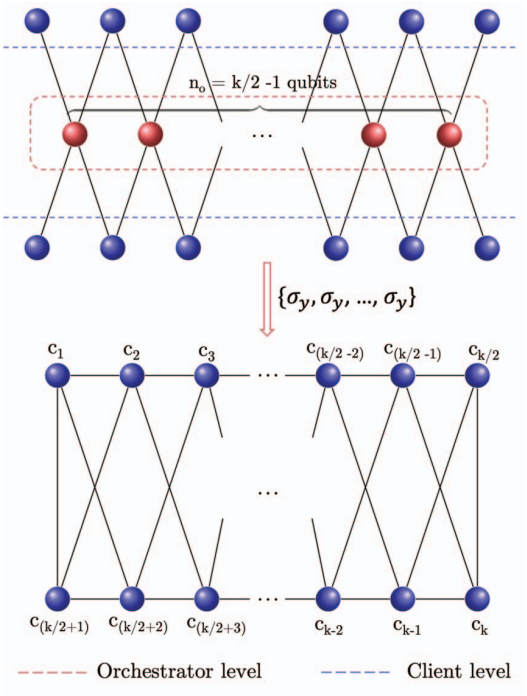

Fig. 5: Generation of an artificial (enhanced) ring topology among the k clients starting from a $(\frac{3}{2}k-1)$-qubit diamond state. In particular, the artificial topology is obtained by (widely) measuring each qubit retained at the orchestrator.

C. From Physical Star Topology to Artificial (Enhanced) Ring Topology

By working on the degrees of freedom introduced in Sec. III-A, a different artificial topology can be built upon the physical star topology. To this aim, we provide the following definition.

Definition 2 (Diamond-like graph state)**.** *We define as "diamond-like graph state" a two-colorable graph state with $n=\frac{3}{2}k-1$ qubits, whose associated graph $G=(V,E)$ is so that:*

$$V = V_A \cup V_B \text{ with } V_A = \{o_i\}_{i=1}^{\frac{k}{2}-1} \ \wedge \ V_B = \{c_i\}_{i=1}^{k} \tag{24}$$

$$E \subset [V]^2 \text{ with } E = \bigcup_{i=1}^{\frac{k}{2}-1} \{\{o_i, c_j\}, \{o_i, c_{\frac{k}{2}+j}\} : j = i, i+1\}$$

Stemming from this entangled resource is possible to built upon the physical star topology an artificial topology among the client nodes, which we refer to as "enhanced ring topology" due to its particular shape, i.e., a ring topology with some extra edges among the nodes. This is possible by performing a number of Pauli σ_y-measurements equal to the number $n_o = \frac{k}{2}-1$ of orchestration vertices, as established by Lemma 2 and shown in Fig. 5.

Lemma 2. *Given a diamond-like graph state with a number of qubits equal to $n=\frac{3}{2}k-1$, with k denoting an even number of clients, then an artificial enhanced ring topology among the k clients can be obtained by performing $n_o=\frac{k}{2}-1$ local Pauli σ_y-measurements on the qubits retained at the orchestrator.*

Proof: The proof follows similarly to Lemma 1, by first applying local complementations of the graph G – associated to the diamond-like graph state – at vertices $\{o_i\}_{i=1}^{n_o}$ and then by deleting these vertices from the resulting graph, as indicated in (12) *and* (13)*. Thus, the artificial topology obtained from the n-qubit diamond-like graph state is expressed via the resulting graph $\tilde{G}_y^{(n_o)}=(V_y,E_y)$ with:*

$$V_y = V \setminus V_A = V \setminus \bigcup_{i=1}^{n_o} \{o_i\} \tag{25}$$

$$E_y = \Big\{\{c_i, c_{i+1}\}, \{c_{\frac{k}{2}+i}, c_{\frac{k}{2}+i+1}\}, \{c_i, c_{k/2+i+1}\}, \{c_{i+1}, c_{k/2+i}\} : i = 1, \dots \frac{k}{2}-1\Big\} \cup \cup \big\{\{c_i, c_{k/2+i}\} : i = 1, \frac{k}{2}\big\}. \tag{26}$$

■

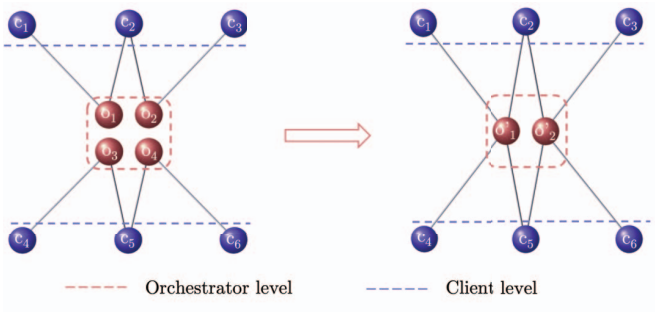

Fig. 6: Diamond-like graph state obtained by locally manipulating at the orchestrator two chain graph states via fusion operations.

We note that Lemma 2 holds for an arbitrary even value of k, and that the number of additional edges among the clients – with respect to the ring topology – is equal to $k-2$. We also observe that a diamond-like graph state can be obtained by generating at the orchestrator two linear cluster states and by performing suitable fusion operations before the distribution, as represented in Fig. 6. Specifically, after the fusion operations and according to Lemma 2, σ_y-measurements on the orchestrator qubits lead to the artificial (enhanced) ring topology.

Remark. *It is evident that an artificial (enhanced) ring topology, with number k of clients greater than 2, allows the extraction of a number of EPR pairs greater than 1 differently from artificial star topologies. Indeed with respect to artificial bus topologies, the enhanced ring provides more degrees of freedom in selecting the identities of the nodes sharing the extracted EPR pairs. Thus, it seems an artificial topology*

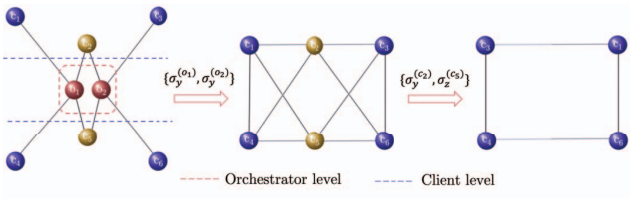

Fig. 7: Pictorial representation of the sequence of Pauli measurements: a) at the orchestrator, for obtaining an artificial enhanced ring topology from a diamond-like graph state, and ii) at the bridges, for eventually obtaining a ring topology.

suitable in contexts characterized by high-variability of the client traffic demands.

Remark. *It is worthwhile to note that the enhanced ring topology can be converted into an artificial ring topology by performing additional Pauli-measurements on the bridge qubits, namely, on the client qubits that are adjacent to more than one orchestrator qubit within the diamond-like graph state. Specifically, as depicted in Fig. 7 for the case $k = 6$, by performing a σ_y-measurement on one of the bridge qubit – say qubit c_2 – followed by a σ_z-measurement on the other one – say qubit c_5 – an artificial ring topology is created.*

IV. Conclusions

In this paper, we have introduced the pivotal role played by multipartite entanglement within Quantum Local Area Network (QLAN) topology. Specifically, we have shown that the engineering of the artificial network topology enabled by multipartite entanglement can be performed on-demand, according to the communication needs, by exploiting only local Pauli measurements at the node responsible for multipartite entanglement generation and distribution. To this aim, we proved that it is possible, by starting from a physical star topology and by wisely manipulating multipartite entanglement, to build different artificial topologies, such as bus, enhanced ring and ring. We hope that this work, by proposing a new perspective on the concept of quantum LANs, will fuel the interest of the community towards QLANs as building block for the future Quantum Internet.

References

[1] A. S. Cacciapuoti, M. Caleffi, F. Tafuri, F. S. Cataliotti, S. Gherardini, and G. Bianchi, "Quantum internet: Networking challenges in distributed quantum computing," *IEEE Network*, vol. 34, no. 1, pp. 137–143, 2020.
[2] W. Dür, R. Lamprecht, and S. Heusler, "Towards a quantum internet," *European Journal of Physics*, vol. 38, no. 4, p. 043001, 2017.
[3] J. Illiano, M. Caleffi, A. Manzalini, and A. S. Cacciapuoti, "Quantum internet protocol stack: a comprehensive survey," *Computer Networks*, vol. 213, 2022.
[4] A. Pirker, J. Wallnöfer, and W. Dür, "Modular architectures for quantum networks," *New Journal of Physics*, vol. 20, no. 5, p. 053054, 2018.
[5] J. Miguel-Ramiro, A. Pirker, and W. Dür, "Genuine quantum networks with superposed tasks and addressing," *npj Quantum Information*, vol. 7, p. 135, 09 2021.
[6] IBM, "Expanding the IBM Quantum roadmap to anticipate the future of quantum-centric supercomputing."
[7] Amazon, "Announcing the AWS Center for Quantum Networking."
[8] A. S. Cacciapuoti, J. Illiano, and M. Caleffi, "Quantum internet addressing," *IEEE Network*, pp. 1–1, 2023.
[9] C. H. Bennett *et al.*, "Teleporting an unknown quantum state via dual classical and einstein-podolsky-rosen channels," *Phys. Rev. Lett.*, vol. 70, pp. 1895–1899, Mar 1993.
[10] A. S. Cacciapuoti, M. Caleffi, R. Van Meter, and L. Hanzo, "When entanglement meets classical communications: Quantum teleportation for the quantum internet," *IEEE TCOM*, vol. 68, no. 6, pp. 3808–3833, 2020. invited paper.
[11] W. Dür, G. Vidal, and J. I. Cirac, "Three qubits can be entangled in two inequivalent ways," *Phys. Rev. A*, vol. 62, p. 062314, Nov 2000.
[12] J. Eisert and H. J. Briegel, "Schmidt measure as a tool for quantifying multiparticle entanglement," *Physical Review A*, vol. 64, July 2001.
[13] M. Hein *et al.*, "Entanglement in graph states and its applications," *arXiv preprint quant-ph/0602096*, 2006.
[14] M. Hein, J. Eisert, and H. J. Briegel, "Multiparty entanglement in graph states," *Physical Review A*, vol. 69, no. 6, p. 062311, 2004.
[15] J. Wallnöfer *et al.*, "Two-dimensional quantum repeaters," *Physical Review A*, vol. 94, no. 5, p. 052307, 2016.
[16] I. Tzitrin, "Local equivalence of complete bipartite and repeater graph states," *Physical Review A*, vol. 98, no. 3, p. 032305, 2018.
[17] S. Bartolucci *et al.*, "Fusion-based quantum computation," 2023.
[18] N. Benchasattabuse, M. Hajdušek, and R. Van Meter, "Architecture and protocols for all-photonic quantum repeaters," *arXiv preprint arXiv:2306.03748*, 2023.
[19] S.-H. Lee and H. Jeong, "Graph-theoretical optimization of fusion-based graph state generation," *Quantum*, vol. 7, p. 1212, Dec. 2023.
[20] W. Kozlowski, S. Wehner, R. V. Meter, B. Rijsman, A. S. Cacciapuoti, M. Caleffi, and S. Nagayama, "Architectural Principles for a Quantum Internet." RFC 9340, Mar. 2023.
[21] R. M. Metcalfe and D. R. Boggs, "Ethernet: distributed packet switching for local computer networks," *Commun. ACM*, vol. 19, p. 395–404, jul 1976.
[22] W. Bux *et al.*, "Architecture and design of a reliable token-ring network," *IEEE JSAC*, vol. 1, no. 5, pp. 756–765, 1983.
[23] N. C. Strole, "The ibm token-ring network — a functional overview," *IEEE Network*, vol. 1, no. 1, pp. 23–30, 1987.
[24] B. Crow *et al.*, "IEEE 802.11 Wireless Local Area Networks," *IEEE Communications Magazine*, vol. 35, no. 9, pp. 116–126, 1997.
[25] M. Epping *et al.*, "Multi-partite entanglement can speed up quantum key distribution in networks," *New Journal of Physics*, vol. 19, p. 093012, sep 2017.
[26] G. Avis, F. Rozpędek, and S. Wehner, "Analysis of multipartite entanglement distribution using a central quantum-network node," *Phys. Rev. A*, vol. 107, p. 012609, Jan 2023.
[27] J. Illiano, M. Caleffi, M. Viscardi, and A. S. Cacciapuoti, "Quantum mac: Genuine entanglement access control via many-body dicke states," *IEEE TCOM*, pp. 1–1, 2023.
[28] H. Shapourian and A. Shabani, "Modular architectures to deterministically generate graph states," *Quantum*, vol. 7, p. 935, Mar. 2023.
[29] H. Aschauer, W. Dür, and H.-J. Briegel, "Multiparticle entanglement purification for two-colorable graph states," *Phys. Rev. A*, vol. 71, p. 012319, Jan 2005.
[30] K. Chen and H.-K. Lo, "Multi-partite quantum cryptographic protocols with noisy ghz states," *Quantum Info. Comput.*, vol. 7, p. 689–715, nov 2007.